

Inhibitory effect of Relatlimab on LAG3-FGL1 interaction investigated by molecular dynamics simulation

Qing Xie(谢晴), Xue-Feng Liu(刘雪峰), Yu-Qing Wang(王雨晴), and Chen-Xiang Wang(王辰祥)
Citation: Chin. Phys. B, 2026, 35 (**4**): 048701. DOI: 10.1088/1674-1056/ae0308
http://cpb.iphy.ac.cn; http://iopscience.iop.org/cpb

What follows is a list of articles you may be interested in

Simulation on mechanochemical coupling of rotary biomotors F_1 and V_1

Liqiang Dai(戴立强), Yao-Gen Shu(舒咬根), and Zhong-Can Ouyang(欧阳钟灿)
Chin. Phys. B, 2026, 35 (**2**): 028702. DOI: 10.1088/1674-1056/ae2674

Molecular dynamics simulations reveal the activation mechanism of human TMEM63A induced by lysophosphatidylcholine insertion

Zain Babar, Junaid Wahid, Xiaofei Ji(季晓飞), Huilin Zhao(赵慧琳), Hua Yu(于华), and Dali Wang(王大力)
Chin. Phys. B, 2025, 34 (**12**): 128704. DOI: 10.1088/1674-1056/ae172d

Mechanical activation of DNA transport across single-walled carbon nanotubes

Junjie Gao(高俊杰), Yichao Wu(吴逸超), Siqi Yu(俞斯棋), Xiaoyan Zhou(周晓艳), and Hangjun Lu(陆杭军)
Chin. Phys. B, 2025, 34 (**10**): 108701. DOI: 10.1088/1674-1056/adce9b

Reconfiguration of B-DNA structure induced by ethanol

Yue Huang(黄悦), Yipeng Chen(陈以鹏), Jing Li(李静), Rongri Tan(谈荣日), and Huanhuan Qiu(邱环环)
Chin. Phys. B, 2025, 34 (**8**): 088707. DOI: 10.1088/1674-1056/adbed9

Effects of palmitoylation on membrane protein partitioning into lipid domains in model cellular membranes

Shishi Wu(吴施施) and Qing Liang(梁清)
Chin. Phys. B, 2025, 34 (**5**): 058701. DOI: 10.1088/1674-1056/adbee9

Inhibitory effect of Relatlimab on LAG3–FGL1 interaction investigated by molecular dynamics simulation

Qing Xie(谢晴), Xue-Feng Liu(刘雪峰)†, Yu-Qing Wang(王雨晴), and Chen-Xiang Wang(王辰祥)

College of Physics, Chengdu University of Technology, Chengdu 610059, *China*

(Received 28 April 2025; revised manuscript received 26 August 2025; accepted manuscript online 4 September 2025)

As immunotherapy becomes increasingly integrated into cancer treatment, LAG3 (lymphocyte activation gene 3) has been recognized as an immune checkpoint that plays an important role in tumor immune evasion. FGL1 (fibrinogen-like protein 1) has been identified as a ligand of LAG3 that mediates immunosuppressive effects through their interaction. While experimental evidence suggests that Relatlimab can block this interaction, the underlying molecular mechanism remains poorly understood. To investigate this, we performed molecular dynamics simulations to analyze the LAG3/FGL1 complex and its interaction with Relatlimab. Our results demonstrate that Relatlimab binding destabilizes the LAG3/FGL1 complex by inducing conformational changes, thereby weakening the overall interaction. Further analysis of key residues reveals that Relatlimab disrupts the LAG3/FGL1 binding, particularly affecting the ARG residues of LAG3 and the GLU and ASP residues of FGL1. These findings provide new insights into the mechanism by which Relatlimab inhibits immune evasion, offering potential for modulating the structure and stability of the LAG3/FGL1 complex. Additionally, we investigated the effect of Favezelimab on the LAG3/FGL1 interaction and observed an effect similar to that of Relatlimab. This study advances our understanding of the roles of Relatlimab and Favezelimab in regulating immune responses and provides valuable theoretical support for the development of cancer therapies targeting the LAG3 signaling pathway.

Keywords: immunotherapy, LAG3, FGL1, Relatlimab molecular dynamics simulations

PACS: 87.15.ap, 87.15.km, 87.15.H–, 87.19.xw

DOI: 10.1088/1674-1056/ae0308 **CSTR:** 32038.14.CPB.ae0308

1. Introduction

With the rapid development of immunotherapy, immune checkpoint inhibitors have emerged as a significant breakthrough in cancer treatment, particularly in enhancing the immune system's ability to target and eliminate tumors.[1–3] The first generation of FDA-approved inhibitors includes antibodies targeting programmed cell death protein 1 (PD-1) and cytotoxic T lymphocyte-associated protein 4 (CTLA-4), which primarily enhance T cell activity by blocking the interaction between these immune checkpoint receptors and their respective ligands.[4] However, despite the efficacy of these antibodies in some patients, particularly in metastatic melanoma, some patients experience toxicity or resistance.[5–7] Therefore, identifying new targets and combining them with existing therapies has become key to improving therapeutic outcomes. In this context, LAG3 (lymphocyte activation gene 3), an emerging immune checkpoint receptor, has gradually attracted the attention of researchers.[8]

LAG3, an important negative immune regulatory molecule, plays a critical role in the activation and maintenance of T cell function.[9,10] Similar to PD-1 and CTLA-4, LAG3 is not expressed in resting T cells but is induced on CD4+ and CD8+T cells after antigen stimulation.[11,12] LAG3 suppresses T cell activity through binding to MHC-II and FGL1, thereby promoting tumor immune evasion, with FGL1 being one of its critical ligands.[13] Relatlimab is a fully human IgG4 monoclonal antibody targeting LAG3, which can simultaneously block the interactions between LAG3 and both MHC-II and FGL1, thereby restoring T cell function. In contrast, Favezelimab primarily exerts its immune-activating effects by blocking the interaction between LAG3 and MHC-II (see Fig. 1).[14–17]

FGL1 is secreted by hepatocytes and is highly expressed in various tumor types such as melanoma, colorectal cancer, and lung cancer.[18–20] It suppresses T cell function by binding to the D1/D2 domain of LAG3, thereby weakening anti-tumor immune responses.[21] Studies have shown that high levels of FGL1 are negatively correlated with the increase of LAG3+T cells and the decrease of CD8+T cells, further confirming its key role in immune evasion.[22] Relatlimab was initially believed to restore T cell function primarily by blocking the interaction between LAG3 and MHC-II.[23] However, recent studies have demonstrated that Relatlimab also effectively disrupts the interaction between LAG3 and FGL1, exhibiting a dual inhibitory mechanism.[16] Compared to blockade of a single pathway, simultaneous inhibition of both LAG3–MHC-II and LAG3–FGL1 interactions may further enhance T cell-mediated anti-tumor immunity. While the mechanism by which Relatlimab interferes with the LAG3–MHC-II pathway has been well characterized, its regulatory effects on the

†Corresponding author. E-mail: liuxuefeng17@cdut.edu.cn

© 2026 Chinese Physical Society and IOP Publishing Ltd. All rights, including for text and data mining, AI training, and similar technologies, are reserved.

LAG3–FGL1 interaction remain poorly understood. Favezelimab, another fully human IgG4 monoclonal antibody targeting LAG3, has not been reported to block the LAG3–FGL1 interaction to date.[17,24] Therefore, this study aims to evaluate the inhibitory effect of Relatlimab on the LAG3–FGL1 interaction and further investigate whether Favezelimab possesses similar activity, providing new mechanistic insights into their potential application in cancer immunotherapy.

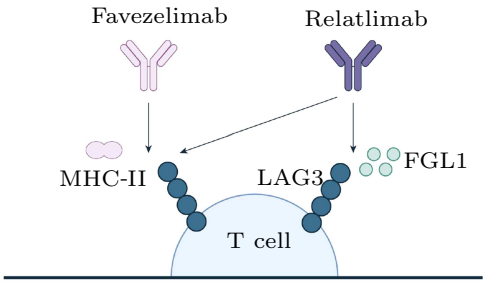


Fig. 1. The diagram illustrates the process by which Relatlimab blocks the interaction between LAG3 and its ligands, MHC II and FGL1. The image shows LAG3 on the surface of the T cell binding to MHC II and FGL1, while Relatlimab blocks its interaction with both ligands. In addition, Favezelimab is also capable of blocking the interaction between LAG3 and MHC II.

In this study, we employed molecular dynamics (MD) simulations and dynamic network analysis to investigate the effects of Relatlimab on the interaction between LAG3 and FGL1. Our results demonstrated that Relatlimab disrupts the LAG3–FGL1 binding interface and enhances the dynamic fluctuations within the complex. We also analyzed Favezelimab to evaluate its potential impact on the LAG3/FGL1 interaction. Relatlimab treatment led to significant alterations in the correlation patterns of the LAG3/FGL1 complex, reflected by marked fluctuations in multiple eigenvalues and increased distribution divergence. MD simulations further revealed that Relatlimab reduced the structural stability and binding integrity of the complex, increased conformational flexibility, and induced substantial dynamic changes. Notably, Relatlimab weakened the binding affinity of key interface residues, particularly by reducing electrostatic interactions, suggesting its role in modulating immune evasion mechanisms. Interestingly, Favezelimab also induced noticeable conformational changes in the LAG3/FGL1 complex, implying its potential to interfere with LAG3–FGL1 binding and modulate LAG3 function. Overall, these findings provide valuable insights into the regulatory mechanisms of Relatlimab and Favezelimab, offering theoretical support for the development of LAG3-targeted immunotherapies. This work highlights new directions for optimizing immune checkpoint inhibitors and advancing precision cancer immunotherapy.

2. Materials and methods

2.1. Protein preparation and molecular docking

We evaluated different assembly strategies for constructing the antibody–LAG-3/FGL1 complex, including docking the antibody to LAG-3 or FGL1 first before introducing the other component. The results of these trials consistently suggested that the binding sites of FGL1 and the antibodies on LAG-3 are distinct and non-overlapping. Based on these observations, and supported by previous studies showing that FGL1 interacts with the D1–D2 domains of LAG-3 through its fibrinogen-like domain (FD), we constructed the LAG-3/FGL1 complex first and subsequently introduced the therapeutic antibodies Relatlimab and Favezelimab.[13] The three-dimensional (3D) protein structures used in this study were obtained from the RCSB Protein Data Bank (RCSB-PDB), with PDB IDs 7TZE and 7TZ2 for LAG3 and FGL1, respectively, and 7UM3 and 6WKM for the inhibitors Relatlimab and Favezelimab.[25] To enhance the accuracy and reliability of molecular docking, all protein structures were preprocessed prior to docking. Structural inspection was performed using Swiss–PdbViewer (SPDBV), and non-essential components such as water molecules, ligands, and small ions were removed. Molecular docking was performed using the PyDOCK online server, where the D1–D2 domain of LAG3 was docked with FGL1 to construct the LAG3/FGL1 complex.[26] Molecular docking generated multiple possible LAG-3/FGL1 conformations. Based on the D1–D2 binding mode reported in the literature and binding free energy calculations, the most energetically favorable conformation was selected as the representative model. For antibody docking, only poses in which Relatlimab and Favezelimab bound to the D1 domain of LAG-3 were retained, from which the final models were selected. As no resolved structure of the LAG3/FGL1 complex is currently available in the PDB database, the docking model was built based on the crystal

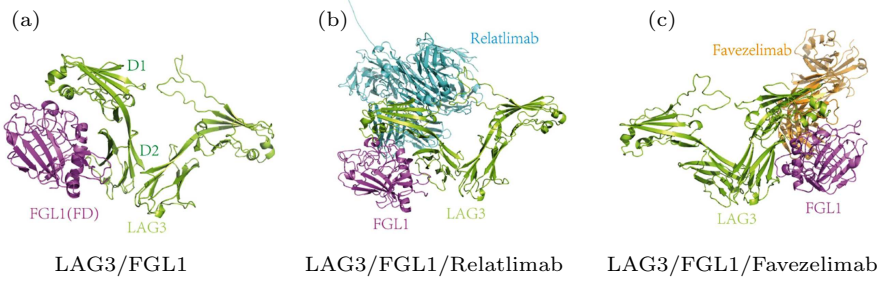


Fig. 2. Protein complex: (a) LAG3/FGL1, (b) LAG3/FGL1/Relatlimab, (c) LAG3/FGL1/Favezelimab. Among them, green represents LAG3, purple represents FGL1, blue represents Relatlimab, and Orange represents Favezelimab.

structure of the FGL1 FD (PDB ID: 7TZ2). Previous studies have shown that the FD domain of FGL1 can specifically interact with the D1–D2 region of LAG3, providing a structural basis for the complex construction.[27] Subsequently, Relatlimab and Favezelimab were docked onto the LAG3/FGL1 complex separately to generate the LAG3/FGL1/Relatlimab and LAG3/FGL1/Favezelimab complexes. The representative structures of the constructed complexes are shown in Fig. 2, highlighting the relative spatial arrangement of LAG3, FGL1, and the antibodies.

Finally, the structural validation of the obtained docking models was conducted using the procheck to ensure the spatial conformation was reasonable and reliable for subsequent molecular dynamics simulations and analyses.[28–30]

2.2. Molecular dynamics simulation

In this study, MD simulations were carried out using the GROMACS 2023 software package, employing the GROMOS96 54A7 force field and the three-point water model.[31,32] The simulation duration was set to 200 nanoseconds with a temperature of 310 K. The complex was positioned at the center of a cubic simulation box, with a minimum distance of 1.0 nm from the box edges. To ensure system neutrality, Na+ and Cl-ions were added. Long-range electrostatic interactions were computed using the Particle Mesh Ewald (PME) method.[33] Energy minimization was performed via the steepest descent method, with a maximum of 50000 iterations. The Berendsen thermostat regulated the temperature at 310 K.[34] The system was first equilibrated in the NVT ensemble for 100 ps, followed by equilibration in the NPT ensemble, where pressure was controlled using the Parrinello-Rahman method.[35] A time step of 2 femtoseconds was employed, and the LINCS algorithm was used to constrain hydrogen bonds.[36] Finally, a 300-nanosecond production simulation was conducted using the same parameters as in the NPT equilibration phase. Three independent 300-nanosecond trajectory simulations were performed for each system, and the final results were obtained by averaging the data from the three trajectories.

2.3. Dynamic cross-correlation matrix analysis

A dynamic cross-correlation matrix (DCCM) analysis was conducted to investigate correlated motions between different regions of the protein. Each amino acid was represented as a node, located at its corresponding Cα atom. Coarse-grained edges were then defined based on residue interactions within the protein complex, reflecting how the protein folds into a specific functional structure.[37] The data for the DCCM analysis were obtained from molecular dynamics simulations and were computed and visualized using the Bio3d plugin from the R package.[38] Molecular dynamics trajectory files were first aligned to remove the effects of global translation and rotation. Atomic fluctuations relative to their average positions were calculated, and these values were used to generate the DCCM, with each matrix element representing the correlation in motion between a pair of atoms.[39] The correlated motion between residues is expressed by the cross-correlation coefficient, which is defined as follows:

$$C_{i,j} = \frac{\langle \delta \boldsymbol{r}_i(t) \cdot \delta \boldsymbol{r}_j(t) \rangle}{\sqrt{\langle (\delta \boldsymbol{r}_i(t))^2 \rangle \langle (\delta \boldsymbol{r}_j(t))^2 \rangle}}. \tag{1}$$

Here, $C_{i,j}$ represents the dynamic correlation between atom i and atom j during the simulation process, where $\delta \boldsymbol{r}_i(t)$ and $\delta \boldsymbol{r}_j(t)$ denote the position vectors of atoms i and j at time t in the simulation, respectively. If the minimum distance between two atoms is less than 4.5 Å, these two residues are considered to be in a contact state and are represented as such in the contact map.

2.4. MM-PBSA calculations

MM/PBSA (Molecular Mechanics/Poisson–Boltzmann Surface Area) is a commonly used method for calculating the binding free energy between a ligand and a receptor in molecular systems.[40] It combines molecular mechanics and solvation effect models to estimate the binding free energy of protein–protein complexes. In this study, we used the AMBER toolkit and the MMPBSA.py script to calculate the binding free energy of LAG3 and the ligand FGL1 in three sets of complexes, followed by energy decomposition to determine the specific contribution of each residue to the free energy.[41] The contributions to the binding free energy are composed of the following terms:

$$\Delta G_{\text{bind}} = \Delta E_{\text{MM}} + \Delta G_{\text{solv}} - T\Delta S, \tag{2}$$

$$\Delta E_{\text{MM}} = \Delta E_{\text{bonded}} + \Delta E_{\text{vdw}} + \Delta E_{\text{ele}}, \tag{3}$$

$$\Delta G_{\text{solv}} = \Delta G_{\text{polar}} + \Delta G_{\text{non-polar}}, \tag{4}$$

where ΔG_{bind} represents the total free energy of the protein–protein complex, ΔE_{MM} reflects the molecular mechanics energy, ΔG_{solv} consists of the free energy of polar solvation and non-polar solvation, and $T\Delta S$ describes the change in the entropy of the degrees of freedom before and after the molecular conformational change.

3. Result

3.1. Docking protein model conformational rationality

To verify the conformational plausibility of the protein complex post-docking, we generated a Ramachandran plot.[42] The Ramachandran plot is a commonly employed method to describe the backbone conformation of a protein, as it displays the φ (phi) and ψ (psi) dihedral angles of each amino

acid residue. Specifically, φ (phi) represents the rotation angle of the C–N bond to the left of the α-carbon in a peptide unit, while ψ (psi) represents the rotation angle of the C–C bond to the right of the α-carbon. In the plot, the distribution within specific regions reflects the conformational characteristics of the protein's secondary structural elements or individual amino acids, while areas outside these regions are typically regarded as forbidden or inaccessible conformational spaces. For the protein complex we docked, the Ramachandran plot showed that more than 97% of the amino acid residues fall within the allowed and additionally the most favored regions, indicating that the resulting docking model exhibits a high degree of structural plausibility and is suitable for further molecular dynamics simulations and analysis. The corresponding Ramachandran plots are provided in The corresponding Ramachandran plots are provided in Figs. S1–S3 of the supplementary materials.

3.2. The stability and conformational changes of protein structure

In this study, we performed a detailed analysis of the molecular dynamics (MD) simulation results of the complex, aiming to investigate the mechanism of action of Relatlimab on the LAG3–FGL1 interaction.[43,44] By calculating the root-mean-square deviation (RMSD) of the complex, we were able to systematically assess the structural stability of the complex during the simulation process. In Fig. 3, we observed that the RMSD values of the LAG3/FGL1/Relatlimab complex and the LAG3/FGL1 complex exhibited smooth variation throughout the entire simlation trajectory, with no significant fluctuations, and both systems stabilized after 50 ns of simulation. This phenomenon suggests that the structure of the complex reached equilibrium during the simulation, rendering the results reliable, further supported by shaded error bands representing standard deviations from independent simulations (see Figs. S13 and S14 of the supplementary materials). Consequently, we selected the simulation trajectory between 250 ns and 280 ns for further analysis.

Further investigation revealed that the average RMSD of the LAG3/FGL1/Relatlimab complex was 0.474 nm, while the average RMSD of the LAG3/FGL1 complex was 0.418 nm. After the simulation reached 60 ns, the RMSD of the LAG3/FGL1/Relatlimab complex remained noticeably higher than that of the control group, indicating that the binding of Relatlimab increased the structural fluctuations of the LAG3/FGL1 complex. More specifically, the binding of Relatlimab may cause a change in the interaction between LAG3 and FGL1, thereby increasing the flexibility of the entire complex and amplifying the dynamic fluctuations of the structure. To further investigate the contribution of residue fluctuations, we analyzed the root-mean-square fluctuation (RMSF) data of the LAG3 residues in the LAG3/FGL1/Relatlimab complex and the LAG3/FGL1 complex. As shown in the plot, the RMSF of the LAG3/FGL1/Relatlimab complex was significantly higher than that of the LAG3/FGL1 complex. The regions marked as box1–box4 in the plot clearly show that the system containing Relatlimab exhibited enhanced fluctuations, consistent with previous studies, indicating that Relatlimab exerts a blocking effect on the LAG3/FGL1 complex, interfering

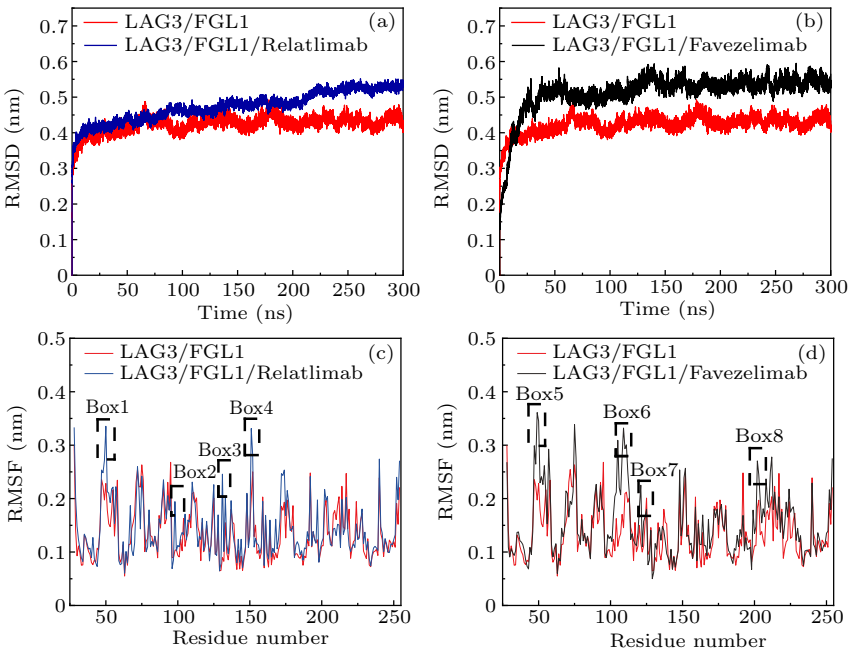


Fig. 3. (a) Root-mean-square deviation (RMSD) of the Cα atoms of LAG3–FGL1 in the LAG3/FGL1 complex and the LAG3/FGL1/Relatlimab complex; (b) RMSD of the Cα atoms of LAG3–FGL1 in the LAG3/FGL1 complex and the LAG3/FGL1/Favezelimab complex; (c) Root-mean-square fluctuation (RMSF) of LAG3 in the LAG3/FGL1 complex and the LAG3/FGL1/Relatlimab complex, where box 1–box 4 represent regions with significant RMSF fluctuations under Relatlimab conditions; (d) RMSF of LAG3 in the LAG3/FGL1 complex and the LAG3/FGL1/Favezelimab complex, where box 5–box 8 represent regions with significant RMSF fluctuations under Favezelimab conditions.

with its stability and increasing the structural fluctuations of the complex. The corresponding difference in RMSF (ΔRMSF) between the LAG3/FGL1/Relatlimab complex and the LAG3/FGL1 complex is shown in Fig. S9 of the supplementary materials. In another set of MD simulations, we analyzed the stability of the LAG3/FGL1/Favezelimab complex. The RMSD of the LAG3/FGL1/Favezelimab complex was also relatively high, suggesting significant perturbation to the LAG3–FGL1 complex. This phenomenon was further validated in the RMSF analysis, where the fluctuations in the box5–box8 regions were notably enhanced. The corresponding ΔRMSF between the LAG3/FGL1/Favezelimab complex and the LAG3/FGL1 complex is shown in Fig. S10.

3.3. Angular changes at LAG3–FGL1 interface

To analyze the dynamic changes at the LAG3–FGL1 interface, the interface angle was used as a descriptor of interfacial conformational changes. Its validity is supported by a positive correlation with solvent-accessible surface area (SASA) (see Fig. S4). The interface angles were then calculated for both the LAG3/FGL1/Relatlimab complex and the LAG3/FGL1 complex.[45] During the simulation, the interface angle was defined by the following atoms: O(Arg121), CA(Phe243), and CB(Trp137). From the figure shown in Fig. 4, it is evident that during the final 100 ns of the simulation, the interface angle of the LAG3/FGL1/Relatlimab complex remained relatively stable, indicating a high level of overall structural stability for the complex and further validating the reliability of the simulation, with the reliability further supported by shaded error bands representing standard deviations from independent simulations (see Figs. S15 and S16). The average interface angle of the LAG3/FGL1/Relatlimab complex was significantly higher than that of the LAG3/FGL1complex, with values of 4.01° and 37.28° for the LAG3/FGL1/Relatlimab and LAG3/FGL1 complexes, respectively. This finding provides additional support for the structural changes induced by Relatlimab upon binding to LAG3–FGL1. The larger interface angle suggests that Relatlimab weakens the interaction between LAG3 and FGL1 by inducing structural changes. In the LAG3–FGL1 bound state, the smaller interface angle indicates a tighter interaction between the two, while the increase in interface angle after Relatlimab binding suggests a reduction in the interaction surface area of the complex, which in turn may affect the binding strength and stability. Furthermore, the increase in interface angle not only implies a weakening of the direct interaction between LAG3 and FGL1, but also suggests that Relatlimab may influence the spatial conformation of the LAG3–FGL1 complex, thereby impacting the overall stability of the complex. Building on this, we further calculated geometric parameters such as interface distance and the number of interfacial residue contacts to more directly evaluate changes in the LAG3–FGL1 interaction.

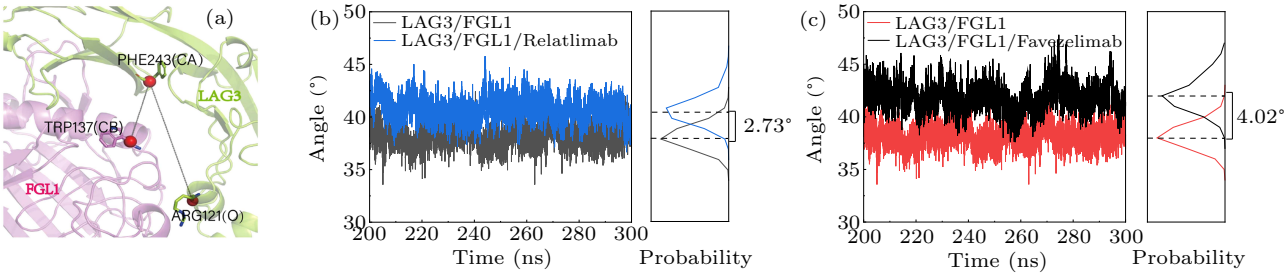


Fig. 4. LAG3–FGL1 interface angle representation: (a) LAG3 is colored in green, and FGL1 is colored in purple. The red spheres represent the selected residues for the interface angle calculation. (b) Interface angle changes of LAG3–FGL1 in the LAG3/FGL1 complex and the LAG3/FGL1/Relatlimab complex. (c) Interface angle changes of LAG3–FGL1 in the LAG3/FGL1 complex and the LAG3/FGL1/Favezelimab complex.

The results showed that, following Relatlimab binding, the distance between LAG3 and FGL1 increased and the number of interfacial contacts decreased, consistent with the observed trend of an increased interface angle (see Figs. S5–S8 in supplementary materials). This conformational change could affect the mode of interaction between LAG3 and FGL1, thereby playing an inhibitory role in immune evasion mechanisms. Additionally, in the LAG3/FGL1/Favezelimab complex, the interface angle also increases upon antibody binding, indicating that Favezelimab induces conformational changes at the binding interface. Consistent with this, the interface distance increases and the number of interfacial contacts decreases, suggesting a weakened interaction between LAG3 and FGL1. These observations mirror the trend seen in the Relatlimab-bound system and further support the hypothesis that Favezelimab may exert its immunomodulatory effect by interfering with the LAG3–FGL1 interaction.

3.4. Dynamic cross-correlation matrix (DCCM) of LAG3–FGL1

To further investigate how Relatlimab affects the interaction between LAG3 and FGL1, we performed a dynamic cross-correlation matrix (DCCM) analysis.[39] DCCM can reveal the dynamic correlations between different residues within a protein. In the DCCM graph, the residue correlation is represented in the form of a color matrix. Specifically, if two residues move in the same direction for the majority of the simulation frames, their correlation is defined as a pos-

itive value, represented in cyan, indicating that their movements tend to change in a synchronized manner. Conversely, if two residues move in opposite directions in most simulation frames, their correlation is defined as a negative value, represented in red, indicating an anti-correlation between their movements. Furthermore, a correlation close to zero suggests that the movement of the residues is nearly uncorrelated or independent.

As shown in Fig. 5, the region corresponding to LAG3 residues 106–228 and FGL1 residues 130–270 exhibits a notable increase in red areas, indicating that Relatlimab weakens the coordinated motion between interface residues and enhances their anti-correlation. This change suggests that Relatlimab significantly alters the dynamic interaction pattern within the complex. A similar pattern was observed in the DCCM of the LAG3/FGL1/Favezelimab complex, further supporting the notion that Favezelimab may exert its immunoregulatory effect by disrupting the dynamic cooperativity of the LAG3–FGL1 interaction. The corresponding ΔDCCM results are provided in Figs. S11 and S12.

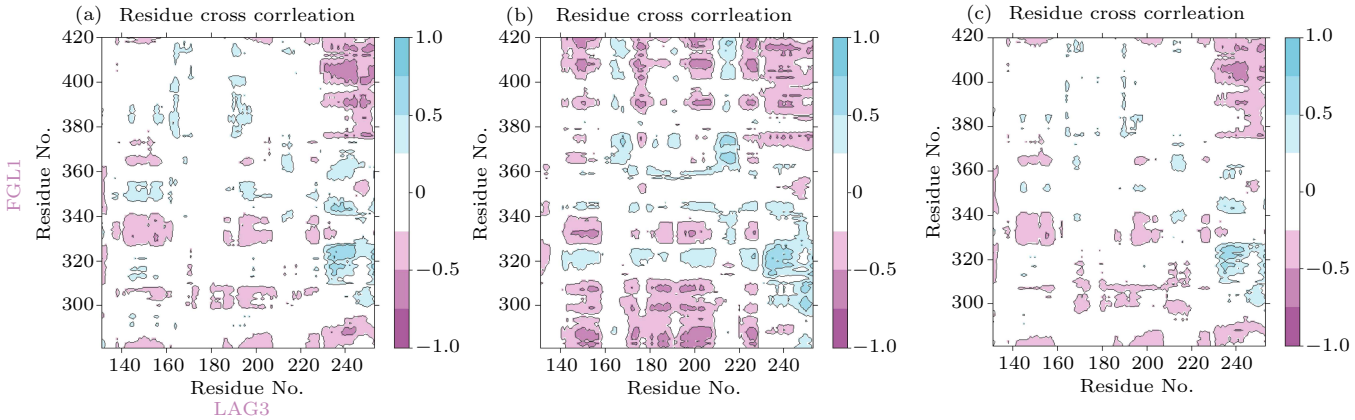


Fig. 5. Panels (a)–(c) respectively show the dynamic cross-correlation matrix of LAG3–FGL1 in the LAG3/FGL1 complex, LAG3/FGL1/Relatlimab complex, and LAG3/FGL1/Favezelimab complex.

3.5. The binding free energy of LAG3–FGL1

To gain a clearer understanding of the effect of the drug on the interaction between LAG3 and FGL1, this study performed the binding free energy (BFE) analysis on both systems at a microscopic level. The mechanism of action of Relatlimab is discussed in detail in the main text, while the related analysis results for Favezelimab are provided in the appendix as supplementary material for reference[46] (see Tables S5–S7). Binding free energy is one of the key parameters used to assess the strength of molecular interactions, and it is primarily composed of van der Waals interactions (VDWAALS), electrostatic energy (EEL), and polar solvation energy (EPB). In this study, we utilized gmx_MMPBSA to calculate the interaction energies between LAG3 and FGL1 in both systems. After extending the simulation to 300 ns, we observed that the system maintained good overall stability over an extended timescale. Given the low energy fluctuations and well-equilibrated state in the later stages of the simulation, we selected the intervals from 250 ns to 280 ns for binding free energy calculations. This choice ensured that the sampled conformations were both statistically independent and representative of the equilibrated ensemble, thereby enhancing the convergence and reliability of the MM-PBSA results. The results (shown in Table 1) showed that the binding free energy of the LAG3/FGL1 complex was −1708.034 kcal/mol, while the binding free energy of the LAG3/FGL1/Relatlimab complex was −1405.624 kcal/mol. This result clearly indicates that the binding free energy of LAG3–FGL1 decreases after Relatlimab binding.

Table 1. The binding free energy was decomposed to a van der Waals interaction ($\Delta E_{\rm vdw}$), electrostatic interaction ($\Delta E_{\rm ele}$), and polar solvation energy ($\Delta G_{\rm solv,PB}$). Energies are in units kcal/mol.

Samples	$\Delta G_{\rm total}$	$\Delta E_{\rm vdW}$	$\Delta E_{\rm ele}$	$\Delta G_{\rm solv}$
LAG3/FGL1	–1708.034	–356.787	–2108.029	756.783
LAG3/FGL1/Relatlimab	–1405.624	–270.401	–1635.304	500.081

The energy component changes in the two systems were further analyzed, and the results showed that the van der Waals interaction energy (VDWAALS) of the LAG3/FGL1/Relatlimab complex was −270.401 kcal/mol, whereas the VDWAALS of the LAG3/FGL1 complex was −356.787 kcal/mol. This difference suggests that Relatlimab binding significantly weakened the van der Waals interaction between LAG3 and FGL1, thereby reducing the stability of the complex. Moreover, the electrostatic interaction energy (EEL) of the LAG3/FGL1/Relatlimab complex was −1635.304 kcal/mol, while the electrostatic energy of the LAG3/FGL1 complex was −2108.029 kcal/mol, indicating that electrostatic interactions play a crucial role in the binding of LAG3 and FGL1. Therefore, in future drug design efforts, disrupting the van der Waals interactions and electrostatic energy between LAG3 and FGL1 will be key for the successful development of inhibitors.

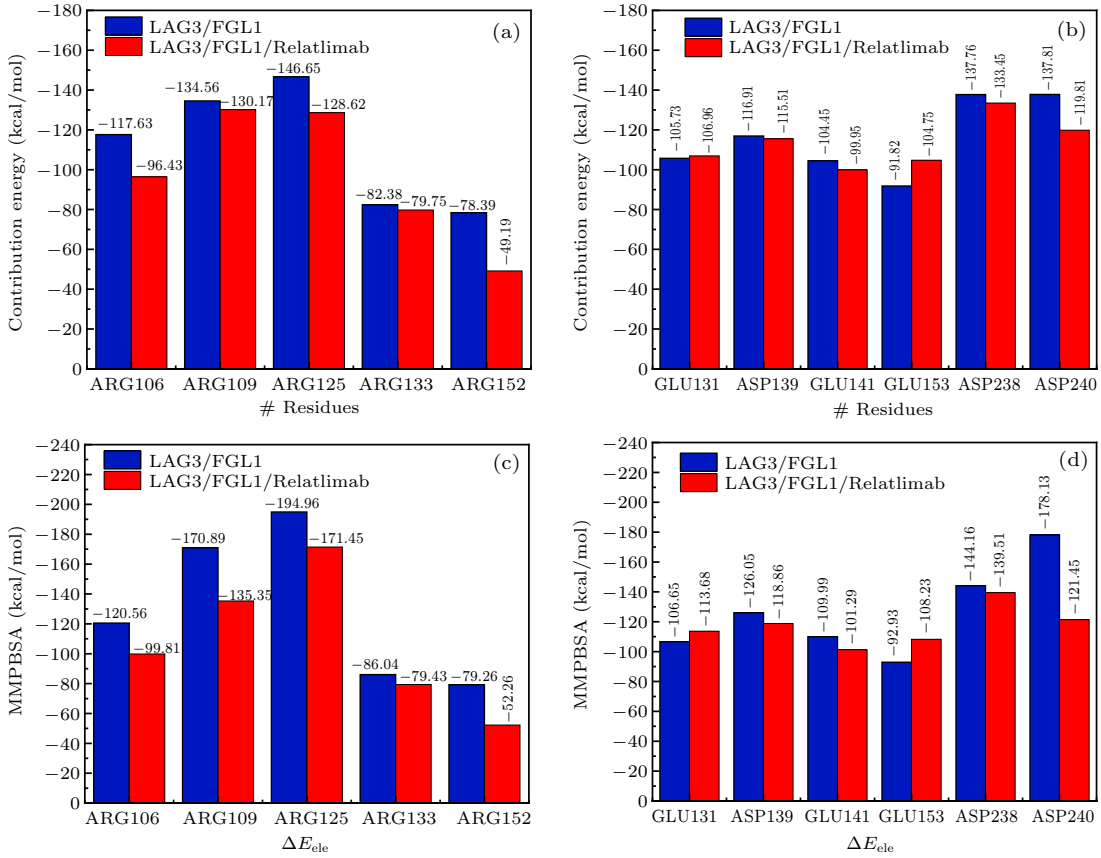


Fig. 6. Panels (a)–(b) respectively show the energy contributions of key residues in LAG3 and FGL1; panels (c) and (d) present the electrostatic interaction analysis of key residues in LAG3 and FGL1. The energy decomposition of each residue was calculated based on the 150 ns–180 ns molecular dynamics trajectory.

As shown in Fig. 6, the energy contributions of individual amino acid residues to the stability of the LAG3-FGL1 complex were analyzed. The analysis revealed that key residues in LAG3 include ARG106, ARG109, ARG125, ARG133, and ARG152, while key residues in FGL1 include GLU131, ASP139, GLU141, GLU153, ASP238, and ASP240. Notably, the core residues mediating LAG3–FGL1 binding in LAG3 are mainly positively charged ARG (arginine) residues and negatively charged GLU (glutamic acid) and ASP (aspartic acid) residues.

Through PyMOL structural analysis, it was found that these key residues are highly concentrated in the D1 binding domain of LAG3, which is crucial for the LAG3–FGL1 interaction. The positively charged side chains of ARG residues are able to form stable electrostatic interactions with the negatively charged GLU and ASP residues on FGL1, promoting stable binding of the complex. Furthermore, the longer side chains of ARG residues can further enhance the stability of the LAG3–FGL1 complex through hydrogen bonding or π–π interactions.

Additionally, we observed a significant decrease in the binding free energy of the key residues in the LAG3/FGL1/Relatlimab complex. This result indicates that Relatlimab may interfere with the interactions of key residues in the LAG3/FGL1 complex, particularly by weakening the electrostatic attraction and hydrogen bond network mediated by ARG residues, thereby reducing the stability of the complex. Clearly, the binding of Relatlimab significantly affects the interaction of the LAG3/FGL1 complex and reduces its stability to some extent, a result consistent with the previous computational analyses. The binding free energy (BFE) analysis further suggests that Relatlimab, by disrupting interactions between key residues, redistributes the energy at the LAG3–FGL1 binding interface, weakening the overall stability of the complex.

Through energy component calculations, we further identified the key residues that contribute most significantly to the binding process. The analysis revealed that key residues on the LAG3 side include ARG106, ARG109, ARG125, ARG133, and ARG152, while key residues on the FGL1 side primarily include GLU131, ASP139, GLU141, GLU153, ASP238, and ASP240. These residues play a core role in the binding interface, especially several ARG residues on the LAG3 side, whose positively charged side chains can form stable electrostatic interactions with GLU and ASP residues on the FGL1 side. In addition, we found that after the binding of Relatlimab, the electrostatic interactions between key residues generally weakened, with ARG109, ARG152, and ASP240 being the most affected. The numerical values of binding free energies and electrostatic interactions are provided in Ta-

bles S1–S4 of the supplementary materials. This further supports the mechanism by which Relatlimab disrupts the electrostatic attraction between critical residues, thereby reducing the stability of the LAG3–FGL1 complex, , with the results further supported by standard deviations from independent simulations (see Figs. S17–S21 of the supplementary materials).

4. Discussion

Although numerous studies have investigated the blocking effect of Relatlimab on the interaction between LAG-3 and MHC-II, its inhibitory effect on the LAG-3/FGL1 interaction remains insufficiently explored.[47,48] To address this gap, we conducted MD simulations to investigate how Relatlimab modulates the LAG-3/FGL1 interaction and thereby impairs immune evasion. Specifically, we simulated both the LAG3/FGL1 complex and the LAG3/FGL1/Relatlimab ternary complex to evaluate the impact of Relatlimab on structural stability. Comparison of the two systems revealed that Relatlimab binding markedly perturbs the stability of the LAG3/FGL1 complex by inducing conformational rearrangements and redistributing interaction energies, ultimately impairing complex formation. These findings offer new insights into the mechanism by which Relatlimab disrupts immune evasion and support its potential as an immunotherapeutic agent.

Root-mean-square deviation (RMSD) analysis showed that the LAG3/FGL1 complex is more stable than the LAG3/FGL1/Relatlimab complex. The addition of Relatlimab significantly increased structural fluctuations, indicating reduced binding stability. As shown in Fig. 3, several regions exhibited elevated flexibility upon Relatlimab binding, further confirming a loss of overall structural integrity. In particular, the interfacial angle between LAG3 and FGL1 increased following Relatlimab binding, leading to weakened direct interactions. Dynamic cross-correlation matrix (DCCM) analysis further revealed that Relatlimab disrupted coordinated motions between key residues at the binding interface, in agreement with the RMSD and structural findings.

To further elucidate the effect of Relatlimab on complex stability, we calculated the binding free energy (BFE) using the MM-PBSA method. As summarized in Table 1, the BFE of the LAG3–FGL1 complex significantly increased upon Relatlimab binding, indicating a decrease in binding affinity. Decomposition of energy contributions showed that both electrostatic interactions and van der Waals forces were weakened, suggesting that Relatlimab alters the energy landscape at the interface. Key residue analysis identified ARG106, ARG109, ARG125, ARG133, and ARG152 of LAG3 and GLU131, ASP139, GLU141, GLU153, ASP238, and ASP240 of FGL1 as critical contributors to the interaction. Notably, the dominant residues in LAG3 were arginine (ARG), while those in FGL1 were predominantly glutamate (GLU) and aspartate (ASP). Electrostatic interactions between these residues were especially important in maintaining complex stability. After the binding of Relatlimab, these key electrostatic interactions were significantly weakened, particularly those involving ARG152, ARG109, and ASP240.

In addition to analyzing the effects of Relatlimab, we also investigated the role of Favezelimab. Previous studies have shown that Favezelimab primarily regulates LAG3 function by modulating its interaction with MHC-II. As such, we examined whether Favezelimab could also influence LAG3 by affecting its interaction with FGL1. Notably, our simulation results indicate that, compared to Relatlimab, Favezelimab has a more pronounced impact on the stability of the LAG3/FGL1 complex. RMSD analysis reveals that Favezelimab binding induces greater structural fluctuations overall, suggesting a stronger destabilizing effect. This is further confirmed by the RMSF analysis, which shows a significant increase in the structural flexibility of LAG3 upon Favezelimab binding. Furthermore, interface angle analysis demonstrates that Favezelimab causes more pronounced changes in the relative orientation between LAG3 and FGL1, which may further weaken their binding affinity. DCCM analysis also indicates that Favezelimab binding reduces the level of coordinated motion between LAG3 and FGL1, suggesting that it disrupts the complex's dynamic behavior to some extent. Taken together, these findings highlight that Favezelimab may regulate LAG3 function by altering its interaction dynamics and structural characteristics with FGL1.

This study elucidates the potential mechanism by which Relatlimab disrupts the LAG3–FGL1 interaction, highlighting its role in weakening key electrostatic interactions and coordinated motions at the interface. Additionally, our simulations suggest that Favezelimab may also exert regulatory effects on this pathway, although experimental evidence is currently lacking and its exact mechanism remains to be clarified. We must acknowledge that this study still has certain limitations. Owing to the lack of direct experimental data on the binding order and dynamic process of LAG-3 and FGL1 *in vivo*, the reliability and generalizability of our simulation results remain limited and require further experimental validation. In future work, we plan to perform systematic in vitro studies, including binding site mutagenesis, competition assays, and affinity measurements, as well as functional studies in animal models, to verify and refine our predictions. In parallel, we aim to resolve high-resolution structures of the LAG-3/FGL1 complex and its antibody-bound states using cryo-electron microscopy, thereby directly testing the interface and conformational changes suggested by our simulations. Through these efforts, we hope to progressively enhance the robustness and biological relevance of our modeling results

and deepen the mechanistic understanding of LAG-3-targeted immunotherapy.

5. Conclusions

This study explored the inhibitory effects of Relatlimab on the LAG3–FGL1 interaction from a molecular dynamics perspective. The results provided new insights into the mechanism of Relatlimab's action in inhibiting immune evasion by inducing structural and energetic changes upon binding. Through molecular dynamics simulations, we found that Relatlimab binding significantly destabilized the LAG3–FGL1 complex. Relatlimab binding induced notable conformational changes and enhanced the structural fluctuations of the complex, thereby weakening the interaction between LAG3 and FGL1. Both RMSD and DCCM analyses consistently showed that Relatlimab binding decreased the dynamic correlation between key residues, resulting in a loss of interface stability. Additionally, binding free energy (BFE) calculations further validated that Relatlimab binding significantly reduced the binding stability of LAG3–FGL1, particularly weakening the van der Waals interactions and electrostatic forces. Notably, the electrostatic energy contribution of key residues in LAG3, especially ARG152, ARG109, and ASP240, decreased significantly after Relatlimab binding, suggesting that Relatlimab mainly disrupts the electrostatic attractions and hydrogen bond network in the LAG3–FGL1 complex, thereby weakening its interaction stability. Building upon our investigation of Relatlimab's inhibitory effect on the LAG3–FGL1 interaction, we further explored the potential impact of Favezelimab. Compared to Relatlimab, Favezelimab binding induced more substantial conformational fluctuations, increased the flexibility of LAG3, and caused greater changes in interface angles. Although the reduction in coordinated motion between key residues was less pronounced than that observed with Relatlimab, DCCM analysis still indicated a certain degree of dynamic disruption. These preliminary results suggest that Favezelimab might influence the LAG3–FGL1 interaction, but its precise mechanism of action requires further investigation and validation.

In conclusion, this study provides insights into how Relatlimab may interfere with the LAG3–FGL1 complex by modulating its conformational dynamics and energy landscape. We also carried out a preliminary exploration of the potential blocking effect of Favezelimab on the LAG3–FGL1 interaction. These findings offer hypothesis-generating structural perspectives that may inform the optimization of LAG3-targeted immunotherapy and guide the development of novel LAG3 inhibitors. Nevertheless, further studies integrating structural biology with biochemical and functional assays will be essential to validate these proposed mechanisms and to support the advancement of optimized LAG3-targeted therapeutics.

Acknowledgement

Project supported by the National Natural Science Foundation of China (Grant No. 11904036).

References

[1] Vafaei S, Zekiy A O, Khanamir R A, Zaman B A, Ghayourvahdat A, Azimizonuzi H and Zamani M 2022 *Cancer Cell International* **22** 1
[2] Mellman I, Coukos G and Dranoff G 2011 *Nature* **480** 480
[3] Schuster M, Nechansky A and Kircheis R 2006 *Biotechnology Journal: Healthcare Nutrition Technology* **1** 138
[4] Rotte A 2019 *Journal of Experimental & Clinical Cancer Research* **38** 255
[5] Abdel-Rahman S A, Rehman A U and Gabr M T 2023 *ACS Medicinal Chemistry Letters* **14** 629
[6] Hao C, Tian J, Liu H, Li F, Niu H and Zhu B 2017 *Medicine* **96** e7325
[7] Indini A, Di Guardo L, Cimminiello C, Prisciandaro M, Randon G, De Braud F and Del Vecchio M 2019 *Journal of cancer research and clinical oncology* **145** 511
[8] Kreidieh F and Tawbi H 2023 *Therapeutic advances in medical oncology* **15** 17588359231186028
[9] Guy C, Mitrea D M, Chou P C, Temirov J, Vignali K M, Liu X, Zhang H, Kriwacki R, Bruchez M P and Watkins S C 2022 *Nature Immunology* **23** 757
[10] Woo S R, Turnis M E, Goldberg M V, Bankoti J, Selby M, Nirschl C J, Bettini M L, Gravano D M, Vogel P and Liu C L 2012 *Cancer Research* **72** 917
[11] Triebel F, Jitsukawa S, Baixeras E, Roman-Roman S, Genevee C, Viegas-Pequignot E and Hercend T 1990 *The Journal of Experimental Medicine* **171** 1393
[12] Liang B, Workman C, Lee J, Chew C, Dale B M, Colonna L, Flores M, Li N, Schweighoffer E and Greenberg S 2008 *The Journal of Immunology* **180** 5916
[13] Wang J, Sanmamed M F, Datar I, Su T T, Ji L, Sun J, Chen L, Chen Y, Zhu G and Yin W 2019 *Cell* **176** 334
[14] Hofmann M, Thimme R and Schamel W W 2024 *Signal Transduction and Targeted Therapy* **9** 291
[15] Cillo A R, Cardello C, Shan F, Karapetyan L, Kunning S, Sander C, Rush E, Karunamurthy A, Massa R C and Rohatgi A 2024 *Cell* **187** 4373
[16] Thudium K, Selby M, Zorn J, Rak G, Wang X, Bunch R, Hogan J, Strop P and Korman A 2022 *Drugs* **82** 1
[17] Garralda E, Sukari A, Lakhani N, Patnaik A, Lou Y, Im S A, Golan T, Geva R, Wermke M and De Miguel M 2022 *ESMO Open* **7** 100639
[18] Liu T Y, Yan J S, Li X, Xu L, Hao J L, Zhao S Y, Hu Q L, Na F J, Li H M and Zhao Y 2024 *Journal of Experimental & Clinical Cancer Research* **43** 213
[19] Chen J, Wu L and Li Y 2024 *Biomarker Research* **12** 53
[20] Li J J, Wang J H, Tian T, Liu J, Zheng Y Q, Mo H Y, Sheng H, Chen Y X, Wu Q N and Han Y 2023 *Nat. Commun.* **14** 6690
[21] Shi A P, Tang X Y, Xiong Y L, Zheng K F, Liu Y J, Shi X G, Lv Y, Jiang T, Ma N and Zhao J B 2022 *Frontiers in immunology* **12** 785091
[22] Qian Y, Sun Y, Shi P, Zhou X, Zhang Q, Dong Q, Jin S, Qiu L, Niu X and Zhou X 2024 *Acta Pharmaceutica Sinica B* **14** 1150
[23] Su J, Fu Y, Cui Z, Abidin Z, Yuan J, Zhang X, Li R and Zhao C 2024 *Frontiers in Pharmacology* **14** 1349081
[24] Timmerman J, Lavie D, Johnson N A, Avigdor A, Borchmann P, Andreadis C, Bazargan A, Gregory G P, Keane C and Tzoran I 2023 *Blood* **142** 4440
[25] Burley S K, Berman H M, Bhikadiya C, Bi C, Chen L, Di Costanzo L, Christie C, Dalenberg K, Duarte J M and Dutta S 2019 *Nucleic Acids Research* **47** D464
[26] Cheng T M K, Blundell T L and Fernandez-Recio J 2007 *Proteins: Structure, Function and Bioinformatics* **68** 503
[27] Ming Q, Celias D P, Wu C, Cole A R, Singh S, Mason C, Dong S, Tran T H, Amarasinghe G K and Ruffell B 2022 *Nat. Immunology* **23** 1031
[28] Lovell S C, Davis I W, Arendall III W B, De Bakker P I, Word J M, Prisant M G, Richardson J S and Richardson D C 2003 *Proteins: Structure, Function and Bioinformatics* **50** 437

[29] Laskowski R A, MacArthur M W, Moss D S and Thornton J M 1993 *Applied Crystallography* **26** 283
[30] Morris A L, MacArthur M W, Hutchinson E G and Thornton J M 1992 *Proteins: Structure, Function and Bioinformatics* **12** 345
[31] Schmid N, Eichenberger A P, Choutko A, Riniker S, Winger M, Mark A E and Van Gunsteren W F 2011 *European Biophysics Journal* **40** 843
[32] Zhang B W, Zhang B Q, Shao Z G and Wu X 2024 *Chin. Phys. B* **33** 118102
[33] Toukmaji A Y and Board Jr J A 1996 *Comput. Phys. Commun.* **95** 73
[34] Berendsen H J, Postma J V, Van Gunsteren W F, DiNola A and Haak J R 1984 *J. Chem. Phys.* **81** 3684
[35] Martoňák R, Laio A and Parrinello M 2003 *Phys. Rev. Lett.* **90** 075503
[36] Hess B, Bekker H, Berendsen H J and Fraaije J G 1997 *J. Comput. Chem.* **18** 1463
[37] Sethi A, Eargle J, Black A A and Luthey-Schulten Z 2009 *Proc. Natl. Acad. Sci. USA* **106** 6620
[38] Grant B J, Rodrigues A P, ElSawy K M, McCammon J A and Caves L S 2006 *Bioinformatics* **22** 2695
[39] dos Santos Nascimento I J, De Souza M, Medeiros D C and de Moura R O 2022 *Medical Sciences Forum* **14** 84
[40] Poli G, Granchi C, Rizzolio F and Tuccinardi T 2020 *Molecules* **25** 1971
[41] Kumari R, Kumar R, Consortium O S D D and Lynn A 2014 *Journal of Chemical Information and Modeling* **54** 1951
[42] Ho B K and Brasseur R 2005 *BMC Structural Biology* **5** 1
[43] Hollingsworth S A and Dror R O 2018 *Neuron* **99** 1129
[44] Michaud-Agrawal N, Denning E J, Woolf T B and Beckstein O 2011 *J. Comput. Chem.* **32** 2319
[45] Wang H, Song L, Zhou T, Zeng C, Jia Y and Zhao Y 2020 *Phys. Chem. Chem. Phys.* **22** 25474
[46] Tuccinardi T 2021 *Expert Opinion on Drug Discovery* **16** 1233
[47] Ibrahim R, Saleh K, Chahine C, Khoury R, Khalife N and Cesne A L 2023 *Biomedicines* **11** 1878
[48] Tawbi H A, Schadendorf D, Lipson E J, Ascierto P A, Matamala L, Castillo Gutiérrez E, Rutkowski P, Gogas H J, Lao C D and De Menezes J J 2022 *New England Journal of Medicine* **386** 24